Evolutionary Ecology Research, 2019, **20**: 27–50

The role of genetic and environmental background driving ontogenetic trajectories of skeletal variation in the threespine stickleback (*Gasterosteus aculeatus* L.)

Alexandra E. Pistore[1], Tegan N. Barry[2], Stevi L. Vanderzwan[2], Heidi Schutz[3], Sean M. Rogers[2] and Heather A. Jamniczky[1]

[1]*Department of Cell Biology and Anatomy, Cumming School of Medicine, University of Calgary, Calgary, Alberta, Canada,* [2]*Department of Biological Sciences, University of Calgary, Calgary, Alberta, Canada and* [3]*Biology Department, Pacific Lutheran University, Tacoma, Washington, USA*

ABSTRACT

Background: Despite their prominence as an evolutionary model, little is known about the developmental trajectories that produce phenotypic differences among threespine stickleback (*Gasterosteus aculeatus*) occupying different habitats. The relationship between shape and size over ontogeny is known to provide an important context for the study of rapid adaptive change.

Objective: Quantify phenotypic variation in skeletal shape and the relationship between shape and size across ontogenetic stages from 90 days post-fertilization to reproductive maturity in stickleback occupying representative habitats.

Methods: We collected wild, reproductively mature fish from marine and freshwater habitats in coastal British Columbia. These were crossed and raised in the laboratory and sampled sequentially for one year. We used 3D geometric morphometrics to quantify the shape of the cranial and postcranial skeleton and to compare ontogenetic trajectories.

Results: Skeletal phenotypes are already distinct by 90 days post-fertilization and remain so throughout ontogeny. The greatest differences occur between freshwater and protected marine habitats. The relationship between shape and size is different for each habitat at each point in time. Ontogenetic trajectories differ among all three habitats, with marine individuals forming more similar trajectories than the those from the freshwater habitat. Our results indicate that genetic differences contribute more strongly to the divergence of freshwater forms from marine forms, while stratification between marine phenotypes is produced by the contribution of developmental timing changes and functional constraints.

Keywords: development, *Gasterosteus aculeatus*, geometric morphometrics, ontogeny, phenotype, skeleton, threespine stickleback.

Correspondence: H.A. Jamniczky, Department of Cell Biology and Anatomy, Cumming School of Medicine, University of Calgary, 3330 Hospital Drive NW, Calgary, AB T2N 4N1, Canada. email: hajamnic@ucalgary.ca

INTRODUCTION

Deciphering the non-linear relationship between genotype and phenotype that produces the extraordinary array of variation present in natural populations requires an understanding of the mechanisms by which genetic information, through development, is translated into morphology under different environmental conditions (Schmalhausen, 1949; Lewontin, 1974). How changes to developmental trajectories might facilitate or constrain the production of novel phenotypic variants upon which selection could act remains a fundamental question of evolutionary developmental biology (Hendrikse *et al.*, 2007; Hallgrimsson *et al.*, 2012; Green *et al.*, 2017). The ability to alter a developmental trajectory may underlie observed differential evolvability among populations, and rapidly changing trajectories may facilitate rapid adaptive radiations (Jamniczky *et al.*, 2015). Alternatively, adaptive change in certain phenotypes may be biased to occur only in specific directions due to the presence of genetic constraints (Schluter, 1996). Further, changes in trajectory origin may indicate the relative contribution of inherited information and developmental timing to trajectory outcomes (Sheets and Zelditch, 2013), while convergent trajectories are thought to indicate the presence of functional constraints (Adams and Nistri, 2010; Simonsen *et al.*, 2017). The relationship between development, form, and evolution thus provides an important link between genetic information and environmental influence on phenotypic variation but is notoriously challenging to test.

The threespine stickleback (*Gasterosteus aculeatus*) is ideal for testing such questions, as the relationship between genotype and phenotype can be studied in the wild as opposed to laboratory settings. Repeated instances of parallel evolution over short periods of time in this taxon provide a unique opportunity to gain insight into the genotype-phenotype-environment interaction space as it acts on organisms on a near-contemporary scale (Bell and Foster, 1994). Extensive work has documented phenotypic traits that differentiate marine and derived freshwater forms (e.g. Hagen and Gilbertson, 1972; Bell, 1976; McPhail, 1993; Walker, 1997; Aguirre and Bell, 2012). Our understanding of the genomic drivers of these morphologies and their appearance under particular selective regimes is growing rapidly (Peichel *et al.*, 2001; Colosimo *et al.*, 2005; Albert *et al.*, 2008; Barrett *et al.*, 2008; Miller *et al.*, 2014; Rennison *et al.*, 2015). Whereas freshwater forms have long been known to be phenotypically more variable than marine forms (e.g. Bell and Foster, 1994; Aguirre and Bell, 2012), recent work indicates that considerable phenotypic and standing genetic variation is also present in marine populations (Morris *et al.*, 2018; T.N. Barry *et al.*, in prep.).

Despite the existence of an annotated genome (Jones *et al.*, 2012; Peichel *et al.*, 2017) and an expanding set of tools for genetic manipulation of this species, information about the timing of the development of divergent morphologies among marine and freshwater stickleback is almost completely absent. Existing work on stickleback morphological development documents only the embryonic period (Swarup, 1958), and fails to capture many aspects of skeletal morphology that develop post-embryonically. A recent study characterizing post-embryonic development of locomotor and armour traits (Currey *et al.*, 2017) provided the first analysis of timing of divergence of some of the more well-studied features that differentiate marine and freshwater forms. This work identified potential roles for both genetic variation and heterochrony in structuring adult phenotypic variation. Previous work has also identified variation in allometric relationships in *G. aculeatus* body shape (Spoljaric and Reimchen, 2011; Wund *et al.*, 2012) and has implicated phenotypic plasticity in the development of derived freshwater forms (Wund *et al.*, 2012).

A gap remains, however, in our understanding of how and when divergence among complex phenotypes arises, and further, of the influence of changing size on the develop-

ment of form in *G. aculeatus*. Because of the need to understand how phenotypes form and how developmental mechanisms such as differential growth produce phenotypic variation while maintaining coordination and performance capacity, and because it is likely that the locus of selection in rapidly changing environments lies at least in part at ontogenetic stages that precede adult, detailed information about ontogenetic trajectories are required to contextualize evolutionary hypotheses.

Here we investigate the ontogeny of skeletal shapes of threespine stickleback originating from three British Columbia habitats: two replicate marine localities and one freshwater lake. We explicitly consider the cranial and locomotor skeletons as a complex, three-dimensional phenotype in order to identify differences in morphology among life stages and quantify the expression of size–shape relationships across ontogeny in different habitats.

METHODS AND MATERIALS

Field collection

Adult threespine stickleback (standard length ≥40 mm *and* exhibiting nuptial colouring, $n = 90$ per locality) were collected in the spring of 2015 from three habitats in southwestern British Columbia, Canada. These included Hospital Bay and Bargain Bay Lagoons considered together due to geographic proximity (49°37′53.4″N, 124°1′48.0″W and 49°36′48.6″N, 124°1′46.9″W respectively), the freshwater, relatively deep, sculpin-free Klein Lake (49°43′45″N, 123°58′06″W) in Madeira Park on the Sunshine Coast, and the marine Roquefeuil Bay (48°51′30″N, 125°06′46″W) on the west coast of Vancouver Island in Barkley Sound. Marine fish were analysed separately by habitat based on our own and others' work (Morris *et al.*, 2018; T.N. Barry *et al.*, in prep.) indicating the presence of substantial genetic and phenotypic variation among marine populations. Furthermore, these marine localities vary substantially in the type of habitat available for stickleback: most notably, the lagoon sites are quiet, protected, and shallow compared with Roquefeuil Bay, which is open to Barkley Sound.

Fish were captured using Gee's minnow traps. Specimens destined for morphometric characterization of adult phenotype ($n = 50$ per locality) were euthanized in the field using an overdose of Eugenol (>400 mg/L (Grush *et al.*, 2004), Sigma-Aldrich). Caudal fin clips were collected and preserved in 70% ethanol; specimens were then fixed flat in 10% neutral buffered formalin for 24 hours, and then placed in 70% ethanol for long-term storage. Specimens destined for laboratory crossing were placed in plastic bags with source water and oxygen overlay ($n = 40$ per locality, 10 fish per transport bag), and transported in a cooler with ice to the Life and Environmental Sciences Centre at the University of Calgary.

Crosses and husbandry

Adult fish were maintained in 120-litre aquaria ($n = 20$ fish per aquarium) at a constant 17°C, with a 16/8 hour light/dark photoperiod, and were acclimated over several weeks to a salinity of 5–6 ppt. They were fed daily with frozen blood worms to satiation. Pure F1 crosses for each habitat were obtained by artificial fertilization. Visual confirmation of reproductive condition was achieved by noting the presence of a bright red throat, blue eyes, marked aggression (males), and abdominal swelling with slight protrusion of eggs

from the urogenital opening (females). Egg masses were extracted manually from reproductive females, which were then elastomer-tagged and returned to their tank. Reproductive males were euthanized as described above, and testes were removed from the abdomen, minced, and mixed with water. This sperm–water mixture was combined with the eggs in a 100×25 mm sterile petri dish and left for ~15 minutes to allow fertilization to occur.

Fertilized egg masses were then covered with a thin layer of E3 growth solution (5 mM NaCl, 0.17 mM KCl, 0.33 mM $CaCl_2$, 0.33 mM $MgSO_4$ in 0.00001% methylene blue) and placed in a 26-litre Percival growth chamber at 18°C and 70% humidity. E3 solution was changed daily, and unfertilized eggs (identified by a lack of membrane formation and neural crest cell migration) were removed after 2–3 days to reduce the potential for fungal contamination. Eggs were maintained in the growth chamber until hatching, at approximately 10 days post-fertilization.

Upon hatching, embryos were transferred to 38-litre aquaria at 17°C, with a 16/8 hour light/dark photoperiod, and a salinity of 5–6 ppt. Hatched embryos were fed brine shrimp larvae twice daily to satiation. Once fish reached 90 days post-fertilization, each family was moved to a 114-litre aquarium, and finely chopped bloodworms were added to their diet. Over several weeks, brine shrimp larvae were replaced with whole bloodworms, and once this transition was completed, feedings were reduced to once daily for the remainder of the study.

Sample composition

Juvenile fish were sacrificed at a series of predetermined times from 5 to 270 days post-fertilization as part of a larger study ($n = 10$ per time point per locality), and euthanized and preserved in 70% ethanol as described above. Complete series for each habitat from ages 90 to 270 days were included in the present analysis (earlier specimens form part of a second study to be reported elsewhere), and each time point sampled contains individuals from several crosses and several tanks, thereby mitigating the possible effects of cross and tank on phenotype.

Sex determination

Caudal fin clips were collected from adult fish and genetic sex was determined using the Isocitrate Dehydrogenase locus (*Idh*) following Peichel *et al.* (2004). Genomic DNA was extracted from fin clips using a DNEasy kit (Qiagen). Polymerase chain reaction (PCR) was run using the primers developed by Peichel *et al.* (2004), and the amplified DNA was run on a 2% w/v agarose gel. Those samples with one band at 302 base pairs were identified as female, and those with two bands at 302 and 271 base pairs were identified as male.

Imaging

Fish were scanned in one of two microcomputed tomography (μCT) instruments, either a Scanco μCT 35 (ScancoAG, Brutisellen, Switzerland) or SkyScan 1173 High Energy MicroCT (Bruker, Kontich, Belgium) system. Specimens were scanned at 70 kV and 114 μA, using 250 projections per 180°, at a voxel size of 20 μm. Fish were scanned in a standardized position, with the mouth closed and the fins and spines held flat against the body wall. Each individual was wrapped in clear plastic wrap and secured with tape to maintain the standardized position and to reduce desiccation in the warm, dry conditions

created by the scanning process. Foam packing was used to further enforce the standardized position and to reduce the potential for movement throughout the scanning process. Scans were conducted from the snout to the distal tips of the pelvic spines. Raw data were imported into Amira 5.4 (Visage Imaging, Carlsbad, CA) to produce 3D reconstructions of the skeleton of each fish, using the isosurface tool with a consistent threshold.

Landmarking

Three-dimensional (3D) landmarks were selected on 159 homologous points on 3D surface models of each fish ranging in age from 90 days post-fertilization to adult (Fig. 1). Adult specimens were landmarked by two observers (A.E.P., T.N.B.), and repeatability between observers was tested using a subset of fish from each habitat before proceeding with the full dataset. Variance attributable to observers was found to be negligible relative to other sources of variance in the dataset (results not shown).

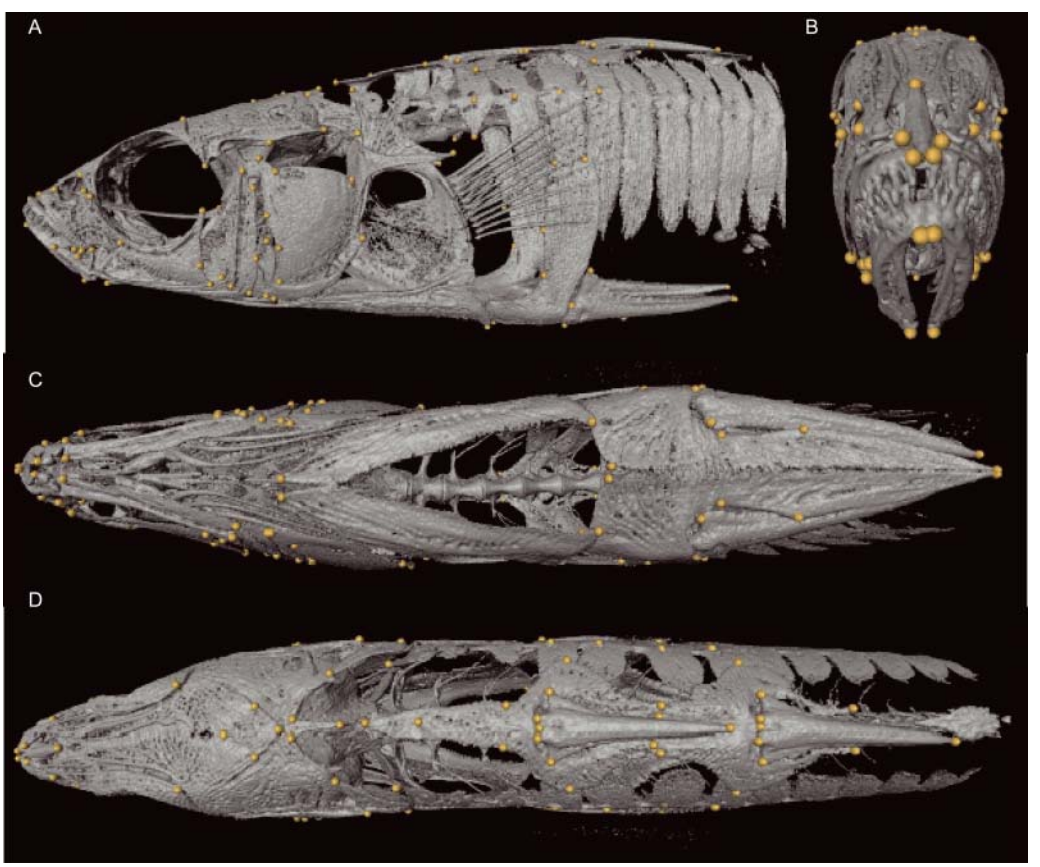

Fig. 1. Three-dimensional landmarks used to quantify skeletal shape on skeletal models of threespine stickleback acquired using microcomputed tomography. This individual is a wild-caught marine adult from Bargain Bay Lagoon, in Madeira Park on the Sunshine Coast of British Columbia. (A) Left lateral view, (B) anterior view, (C) inferior view, (D) superior view.

Shape analyses

Raw landmark data were aligned using Generalized Procrustes Superimposition to remove artifacts produced by scale, rotation, and translation (Dryden and Mardia, 1998). Linear models and non-parametric multivariate analyses of covariance (np-MANCOVA) (Collyer *et al.*, 2015) were used to evaluate the relative contributions of size, habitat, and sex (adult only) to shape variance at each age. This method, which makes use of residual randomization in permutation procedures (Collyer *et al.*, 2018) has been shown to be robust for high-dimensional datasets such as those described here, where the number of landmarks collected exceeds the number of individuals landmarked (Collyer *et al.*, 2015). Effect sizes for these analyses, reported as *Z*-scores, were calculated as standard deviations of the *F*-distribution (Collyer and Adams, 2013).

Although it is well understood that allometric effects contribute a large proportion of variance in nearly all studies of animal shape, it is also important to note that the relationship between shape and size contains an important biological signal. Therefore, attempting to control for the effects of allometry in a dataset in order to visualize shape change, using such techniques as multivariate regression, may have unintended consequences for shape analyses when a common allometry does not exist among the groups being compared. Consequently, we used a Homogeneity of Slopes test to determine if allometry affects shape in the same way for each habitat (Adams and Nistri, 2010), and confirmed that the relationship between shape and size (represented here as the natural log of landmark configuration centroid size) differed among habitats at every age (see Results). Additionally, after accounting for size in a linear model, habitat remained a significant main effect in all cases. As a result, we chose to retain size as a contributing component in our visualizations of shape change. Principal components analysis (PCA) was used to identify major axes of variation in each dataset and to visualize shape changes associated with these axes. We produced a visualization of the differences in relationship between shape and size among habitats at each age by plotting the first principal component of the predicted values from a regression of shape on size against the natural log of centroid size (Adams and Nistri, 2010). These regressions were performed separately for each habitat.

Phenotypic trajectory analysis (Adams and Collyer, 2009; Collyer and Adams, 2013; Sheets and Zelditch, 2013) was used to visualize shape changes over the entire ontogenetic series described here and to more thoroughly explore the developmental pathway that allows each population to arrive at its distinctive adult phenotype. In this analysis, size was included as a covariate in order to account for changing size over time, and the shapes of the paths produced by shape change over ontogeny in each habitat were compared pair-wise to determine if differences existed between the ontogenetic trajectory of fish from each habitat. We also produced another shape–size plot, as described above, for the entire ontogenetic series as an alternate method of visualizing allometry over time in each habitat.

All geometric morphometric analyses were conducted using R v.3.5.0 (R Core Team, 2018) running under RStudio v.1.1.453 (R Core Team, 2016), and the tools contained in the packages geomorph v.3.0.6 (Adams *et al.*, 2018) and plyr v.1.8.4 (Wickham, 2011). All significance testing was carried out using a randomized residual permutation approach with 1000 permutations.

Ethics statement

All collection, husbandry, and euthanasia procedures were conducted in accordance with the Canadian Council for Animal Care, and permitted by the British Columbia Ministry of

Forests, Lands, and Natural Resources Operations, and Fisheries and Oceans Canada (AC12-0057; 15-0108FR; MRSU15-168710; FIL2015-0029; XR109-2015).

RESULTS

Allometric patterns are not shared across habitats

A linear model for the complete dataset including centroid size as a covariate and habitat as a main effect revealed a significant effect of size on shape ($P = 0.001$, Table 1). The significant interaction between size and shape ($P = 0.001$, Table 1) indicated that there is no common allometric component in the dataset. Pairwise comparisons showed that all slopes differ from each other (all $P = 0.01$), and we first present a comparison of phenotypes and allometric patterns at each time point before further considering the complete dataset.

Allometric relationships change across ontogeny as phenotypes approach adult morphology

90 days post-fertilization

At 90 days post-fertilization (dpf), a linear model including centroid size as a covariate and habitat as a main effect revealed that there are significant effects of size and habitat on shape, and that the interaction between size and habitat is also significant (Table 2). Pairwise comparisons of mean shape indicate significant differences ($P = 0.01$) among all three habitats (representative morphologies are presented in Fig. 2), with the greatest difference occurring between freshwater and Madeira Park marine fish. Principal components analysis of the 90 dpf dataset (Fig. 3A indicates that shapes are already clustering by habitat, with

Table 1. Non-parametric multiple MANCOVA results for the complete dataset

	df	SS	MS	*F*	*Z*	*P*
Log(Csize)	1	0.281	0.281	86.164	10.160	0.001
Habitat	2	0.358	0.179	54.949	12.714	0.001
Log(Csize) × Habitat	2	0.042	0.021	6.367	9.656	0.001
Residuals	267	0.871	0.003			

Abbreviations: log(Csize) = natural log of centroid size; *df* = degrees of freedom; SS = sum of squares; MS = mean square; *F* = *F*-statistic; *Z* = effect size, *P* = alpha value.

Table 2. Non-parametric multiple MANCOVA results for the 90 days post-fertilization dataset

	df	SS	MS	*F*	*Z*	*P*
Log(Csize)	1	0.013	0.013	5.038	3.530	0.001
Habitat	2	0.075	0.037	14.993	7.026	0.001
Log(Csize) × Habitat	2	0.007	0.003	1.455	4.672	0.001
Residuals	31	0.077	0.002			

Abbreviations: log(Csize) = natural log of centroid size; *df* = degrees of freedom; SS = sum of squares; MS = mean square; *F* = *F*-statistic; *Z* = effect size, *P* = alpha value.

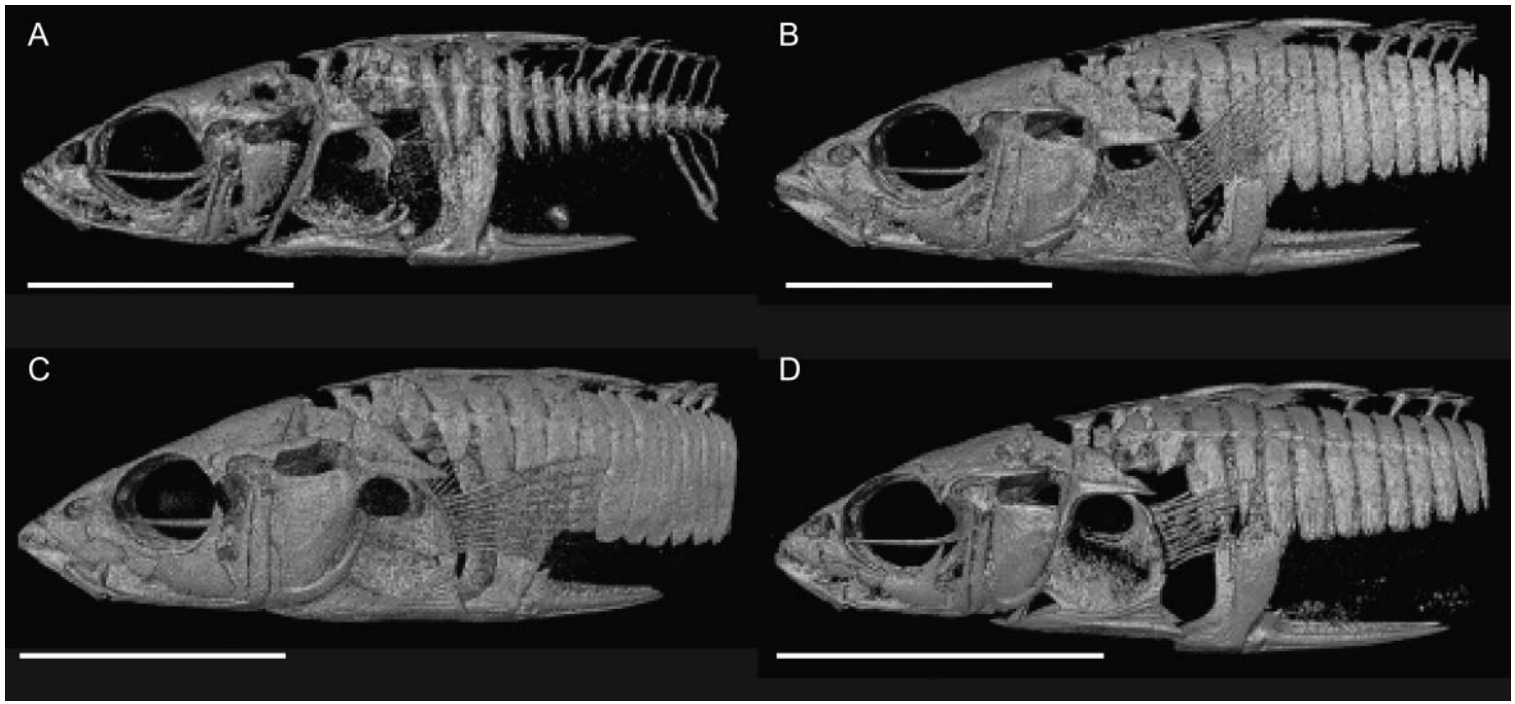

Fig. 2. Comparison of skeletal shape and ossification for threespine stickleback raised in a common freshwater environment for 90 days from three British Columbia habitats. (A) and (B) are specimens from Madeira Park, demonstrating the range of variation present in this habitat; (C) a specimen from Roquefeuil Bay and (D) a specimen from Klein Lake. Scale bar = 10 mm.

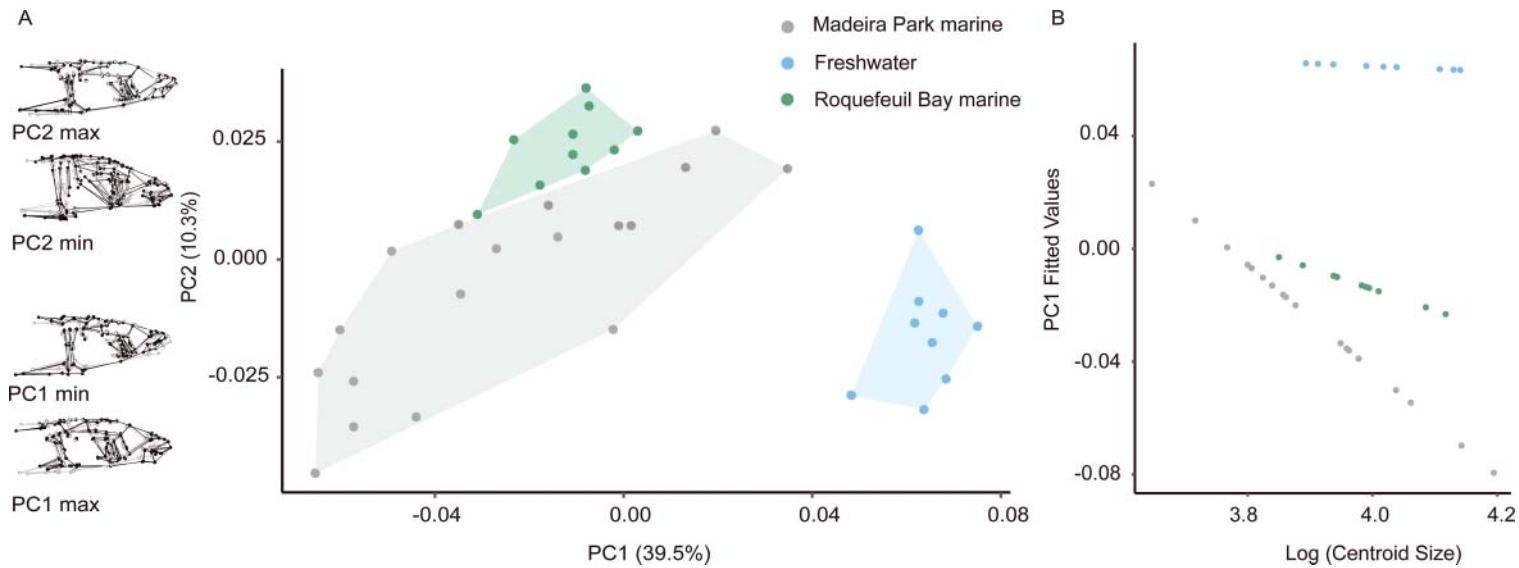

Fig. 3. Principal components analysis and allometric trends for juvenile threespine stickleback at 90 days post-fertilization. Dark wireframe shapes indicate maximum deviation from grey mean shapes for the whole dataset. Abbreviations: dpf = days post-fertilization; Log = natural log; PC = principal component.

the freshwater representatives separate from the other two groups along PC1. The Madeira Park marine group overlaps the Roquefeuil Bay marine group at the positive end and the freshwater group towards the negative end of the axis, and is notable for occupying a much larger area of morphospace, indicating much greater phenotypic variation in the Madeira Park marine habitat relative to the other two habitats. Shapes located towards the positive end of PC1 (freshwater) exhibit relatively shorter pelvic spines, a dorsoventrally reduced girdle region, and a deeper cranial skeleton with large eyes. The negative end of PC1 (marine) represents elongated pelvic spines, a fusiform body shape, and a relatively compact opercular region. Shapes located towards the positive end of PC2 (marine) are more elongated overall with a recognizably marine shape, whereas shapes located towards the most negative end of PC2 (Madeira Park marine) are antero-posteriorly shortened, broader in the girdle region, and have a substantially reduced orbital area.

Figure 3B describes the relationship between shape and size across all three habitats at 90 dpf. The Madeira Park marine group demonstrates a strong relationship between shape and size and a relatively large amount of size variation relative to shape, whereas the Roquefeuil Bay marine group shows a weaker relationship that is vertically displaced and includes far less size variation, and the freshwater group an even further vertically displaced and almost non-existent relationship between shape and size.

180 days post-fertilization

At 180 dpf, a linear model including centroid size as a covariate and habitat as a main effect revealed that there are significant effects of size and habitat on shape in this dataset, and that the interaction between size and habitat is also significant ($P = 0.001$, Table 3). Pairwise comparisons again indicate significant differences ($P = 0.001$) in mean shapes among all three groups, with the greatest difference occurring between Madeira Park marine and freshwater fish. Principal components analysis of the 180 dpf dataset (Fig. 4A) indicates clustering by habitat, with the freshwater group again separate from the other two groups along PC1. PC2 now separates the marine habitats from each other, with the freshwater group overlapping the other two groups on this axis. All three groups occupy approximately the same amount of morphospace at this timepoint. Shapes occupying the positive end of PC1 (freshwater) exhibit highly reduced pelvic spines, and an oval body shape that tapers at both anterior and posterior extremes, and notably enlarged eyes and facial skeleton. Fish occupying the negative end of PC1 (marine) are distinctly fusiform with relatively elongated and enlarged pelvic spines and a substantially reduced facial skeleton. The

Table 3. Non-parametric multiple MANCOVA results for the 180 days post-fertilization dataset

	df	SS	MS	*F*	*Z*	*P*
Log(Csize)	1	0.020	0.020	7.845	4.818	0.001
Habitat	2	0.063	0.031	12.359	7.848	0.001
Log(Csize) × Habitat	2	0.007	0.004	1.555	4.391	0.001
Residuals	34	0.086	0.003			

Abbreviations: log(Csize) = natural log of centroid size; *df* = degrees of freedom; SS = sum of squares; MS = mean square; *F* = *F*-statistic; *Z* = effect size, *P* = alpha value.

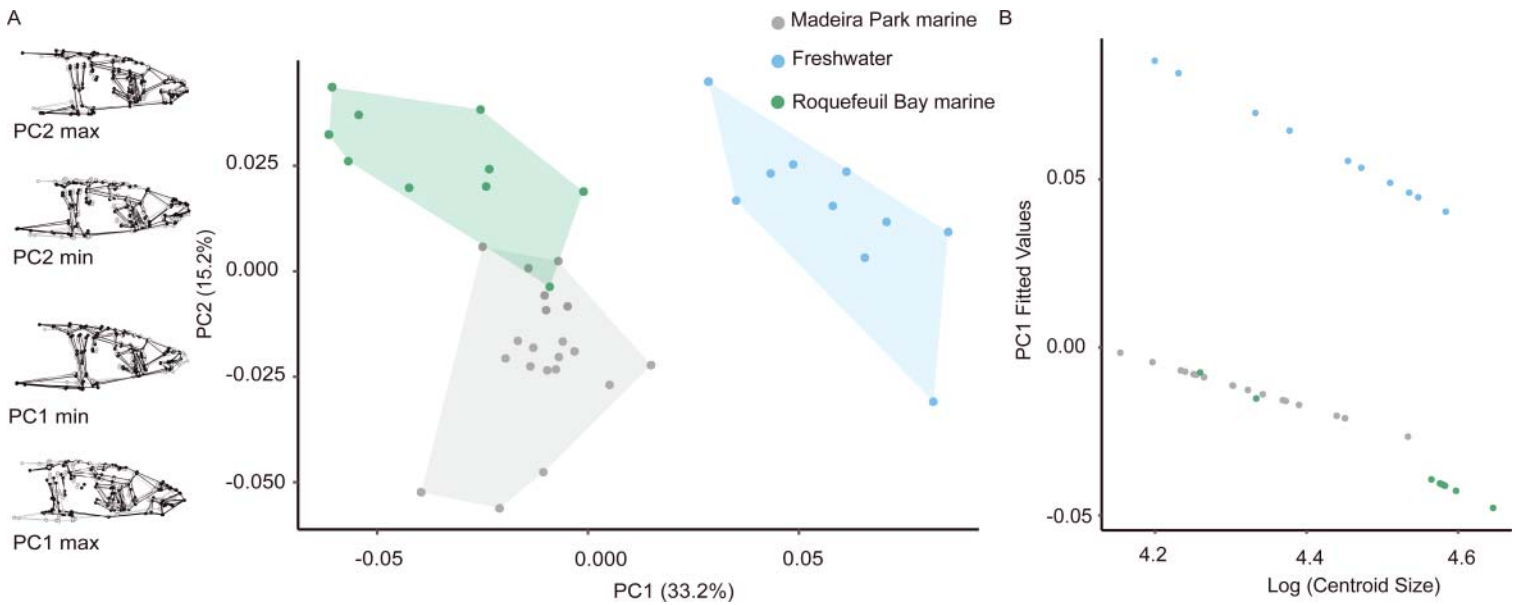

Fig. 4. Principal components analysis and allometric trends for juvenile threespine stickleback at 180 days post-fertilization. Dark wireframe shapes indicate maximum deviation from grey mean shapes for the whole dataset. Abbreviations: dpf = days post-fertilization; Log = natural log; PC = principal component.

positive end of PC2 (freshwater and Roquefeuil Bay marine) includes shapes with elongated dorsal spines, slightly reduced pelvic spines accompanied by elongate dorsal spines, and a slight dorsoventral enlargement of the posterior cranial skeleton. Shapes occupying the negative end of PC2 (Madeira Park marine) have notably enlarged and elongated pelvic spines, larger eyes, a more vertically oriented opercular skeleton, and reduced oral jaws.

Figure 4B describes the relationship between shape and size across all three habitats at 180 dpf. In contrast to the 90 dpf dataset (Fig. 3B), the marine groups exhibit parallel and overlapping allometric slopes, whereas the freshwater group exhibits a parallel but vertically displaced slope.

270 days post-fertilization

At 270 dpf, a linear model including centroid size as a covariate and habitat as a main effect revealed that there are significant effects of size and habitat on shape in this dataset ($P = 0.001$, Table 4), and that the interaction between size and habitat is also significant ($P = 0.022$, Table 4). Pairwise comparisons indicate significant differences ($P = 0.01$) in mean shape among all three groups, with the greatest differences again occurring between freshwater and Madeira Park marine groups. Principal components analysis of the 270 dpf dataset (Fig. 5A) once again indicates clustering by habitat following the same general pattern as at 180 dpf (Fig. 4A). Once again, the Madeira Park marine group occupies a larger amount of morphospace relative to the Roquefeuil Bay marine and freshwater groups. Shapes occupying the positive end of PC1 (freshwater) are discoid in shape with highly reduced pelvic and pectoral skeletons, shortened dorsal spine, broadened posterior cranium, and substantially enlarged oral and facial skeletons. Shapes occupying the negative end of PC1 (marine) are fusiform with reduced facial and oral skeletons, and an enlarged girdle region. The positive end of PC2 (Madeira Park marine) includes shapes with a relatively deeper girdle region and slightly reduced dorsal spines, while the negative end of PC2 (Roquefeuil Bay marine) includes shapes with short but robust pelvic spines, a compact girdle region, and slightly narrower posterior cranium. The freshwater group occupies a middle position along PC2.

All three groups indicate a similar strong relationship between size and shape (Fig. 5B), with the trajectories for the marine groups crossing each other at the midpoint whereas the freshwater trajectory is again vertically displaced.

Table 4. Non-parametric multiple MANCOVA results for the 270 days post-fertilization dataset

	df	SS	MS	*F*	*Z*	*P*
Log(Csize)	1	0.036	0.036	14.035	5.751	0.001
Habitat	2	0.045	0.022	8.719	7.699	0.001
Log(Csize) × Habitat	2	0.004	0.002	0.854	1.987	0.022
Residuals	34	0.087	0.003			

Abbreviations: log(Csize) = natural log of centroid size; *df* = degrees of freedom; SS = sum of squares; MS = mean square; *F* = *F*-statistic; *Z* = effect size, *P* = alpha value.

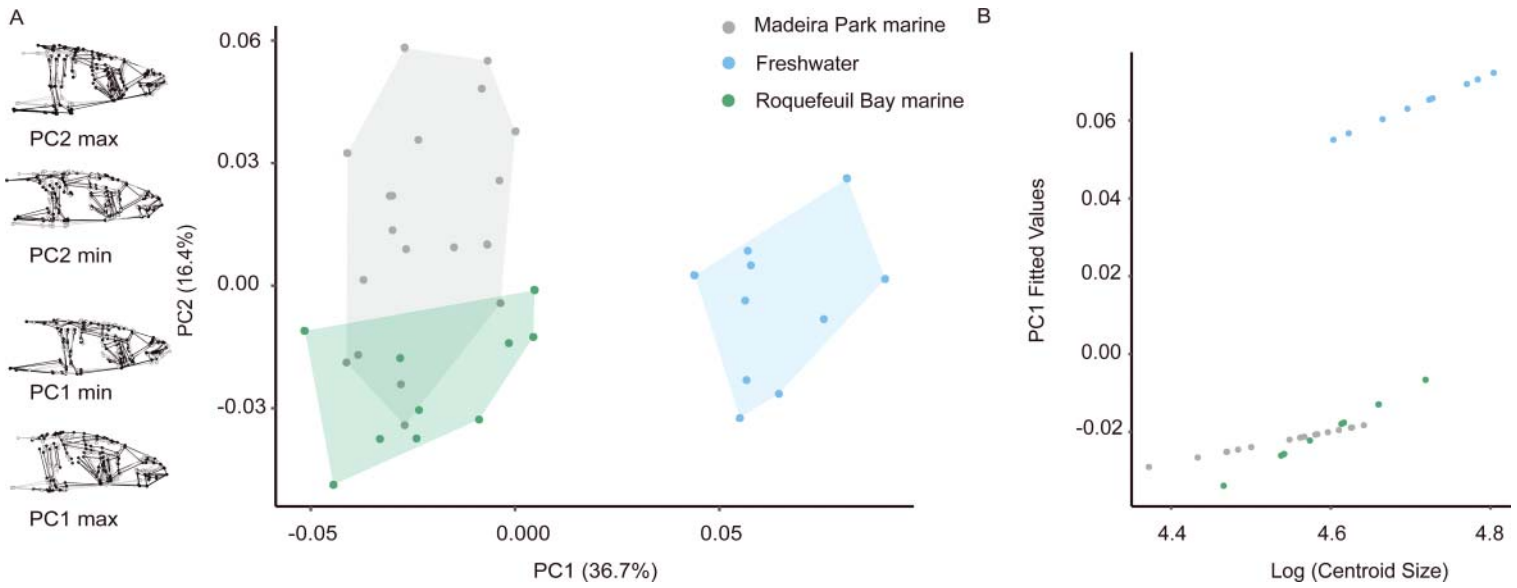

Fig. 5. Principal components analysis and allometric trends for juvenile threespine stickleback at 270 days post-fertilization. Dark wireframe shapes indicate maximum deviation from grey mean shapes for the whole dataset. Abbreviations: dpf = days post-fertilization; Log = natural log; PC = principal component.

Adults

A linear model including centroid size as a covariate and both habitat and sex as additional main effects revealed that there are significant effects of size, habitat, and sex on shape for adults ($P = 0.001$, Table 5), and further that significant interactions are present between all three model terms ($P = 0.001$ except size × sex where $P = 0.019$ and size × habitat × sex where $P = 0.006$, Table 5). Pairwise comparisons among mean shapes reveal that all three habitats differ significantly from each other ($P = 0.001$), with the largest differences in mean shapes again occurring between freshwater and Madeira Park marine groups. Principal components analysis of the adult dataset (Fig. 6A) indicates that shapes cluster by habitat without overlap along PC1, with the freshwater and Madeira Park marine individuals occupying substantially more morphospace than the Roquefeuil Bay marine group. Additionally, the Roquefeuil Bay marine group occupies an intermediate position between the freshwater and Madeira Park marine groups along this axis. Shapes occupying the positive end of PC1 (freshwater) exhibit highly reduced dorsal and pelvic spines, a dorsoventrally narrowed girdle, a rectangular cranial skeleton, and an enlarged opercular and facial region with a very large orbit. Shapes occupying the negative end of PC1 (Madeira Park marine) exhibit elongate and robust pelvic spines, a dorsoventrally expanded girdle, and reduced oral and facial skeleton with a smaller orbit.

Morphospace occupation along PC2 is extensive with overlap among all three groups, representing variation most closely linked to sex. Males tend to occupy the positive end of their group's distribution along this axis with a comparatively gracile girdle and a fusiform cranial skeleton. In contrast, females tend to occupy the negative end of their group's distribution along this axis, with an even more streamlined fusiform shape, a shortened facial skeleton, antero-posteriorly compressed opercular region, and especially long pelvic spines accompanying a dorsoventrally shortened girdle. This phenotype most strongly defines the Roquefeuil Bay marine females. Several outlier individuals in each habitat cluster with members of the opposite sex within their habitats, and the effect of sexual dimorphism appears most pronounced in fresh water (although sample size may be biasing this result; see Discussion). This graphical representation supports our statistical finding of both a major effect of sex and a substantial sex × habitat interaction (Table 5), indicating

Table 5. Non-parametric multiple MANCOVA results for the adult dataset

	df	SS	MS	*F*	*Z*	*P*
Log(Csize)	1	0.171	0.171	65.211	9.372	0.001
Habitat	2	0.121	0.060	22.950	11.539	0.001
Sex	1	0.048	0.048	18.270	10.026	0.001
Log(Csize) × Habitat	2	0.012	0.006	2.235	6.265	0.001
Log(Csize) × Sex	1	0.003	0.003	1.005	2.350	0.019
Habitat × Sex	2	0.008	0.004	1.516	4.491	0.001
Log(Csize) × Habitat × Sex	2	0.006	0.003	1.129	3.281	0.006
Residuals	144	0.379	0.003			

Abbreviations: log(Csize) = natural log of centroid size; *df* = degrees of freedom; SS = sum of squares; MS = mean square; *F* = *F*-statistic; *Z* = effect size, *P* = alpha value.

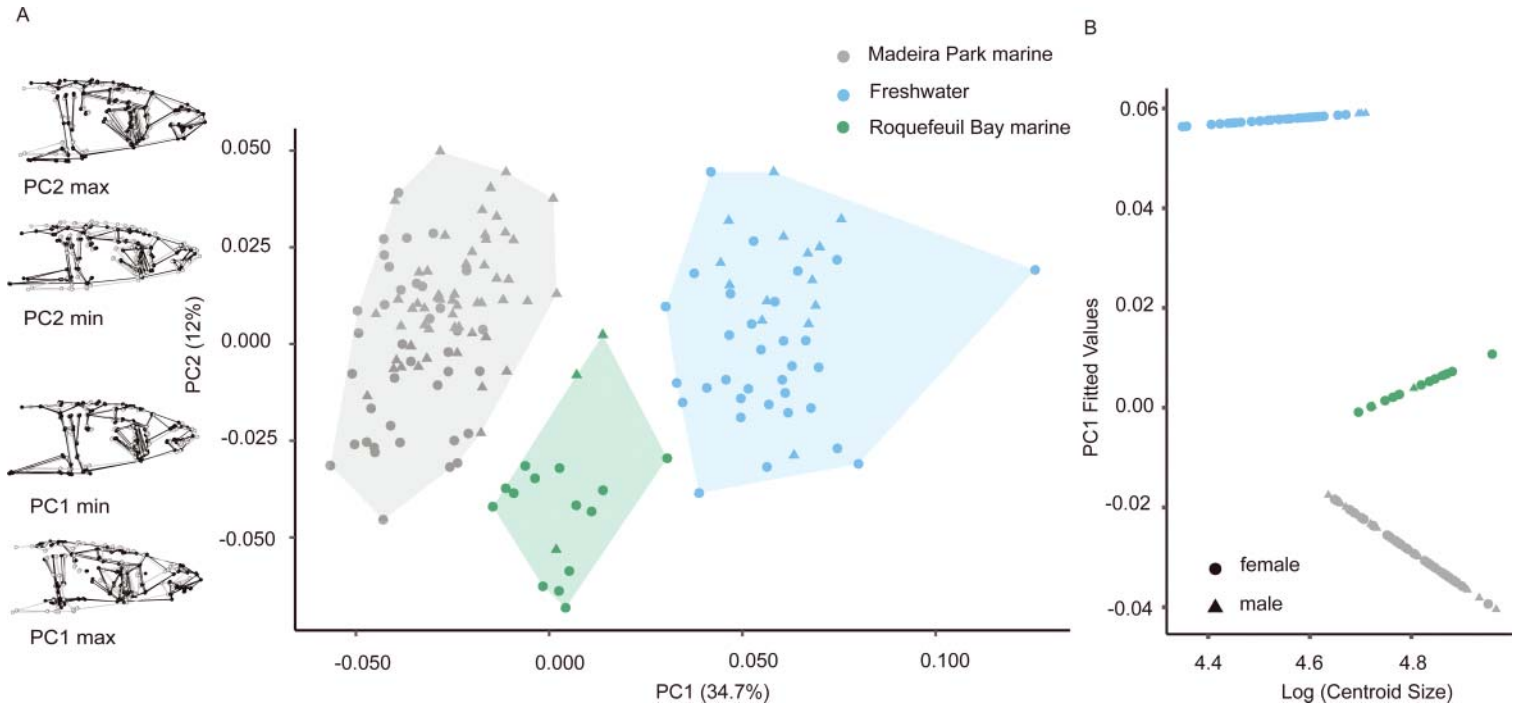

Fig. 6. Principal components analysis and allometric trends for reproductively mature wild-caught adult threespine stickleback. Dark wireframe shapes indicate maximum deviation from grey mean shapes for the whole dataset. Abbreviations: dpf = days post-fertilization; Log = natural log; PC = principal component.

that sexual dimorphism is present in all three habitats but is differentially expressed. A complex pattern is apparent in the relationship between shape and size at this time point (Fig. 6B). All three habitats differ substantially in their shape–size relationships, with the Roquefeuil Bay marine group demonstrating an inverse relationship to those exhibited by the Madeira Park marine and freshwater fish. All three groups are vertically displaced from each other, and the relationship between shape and size in the freshwater group is much weaker than in the marine groups.

Ontogenetic trajectories differ for all three habitats

Phenotypic trajectory analysis with size included in the model as a covariate revealed that the marine habitats follow similar, but not identical, paths through morphospace as they arrive at their adult morphologies, whereas the freshwater habitat begins in, travels through, and ends in an entirely different region of morphospace (Fig. 7A). Pairwise comparisons demonstrate different shapes ($P = 0.05$) and different vector correlations (orientations in morphospace; $P = 0.005$) for all three trajectories. The Roquefeuil Bay marine trajectory differs in length from the Madeira Park marine and freshwater trajectories ($P = 0.02$), but the latter do not differ from each other. All three trajectories generally indicate most change along PC2 (given that size is likely a large contributor to PC1, variance due to size has been accounted for in this analysis), but notably the Roquefeuil Bay marine trajectory contains a period in which substantial change along PC1 occurs in concert with near stasis along PC2, leading to a termination point that is displaced from that of the Madeira Park marine trajectory. It is also notable that the freshwater trajectory indicates near stasis in morphology between 270 dpf and adulthood, while the marine groups exhibit substantial change during this period.

A plot of the first principal component of the fitted values of the entire dataset against the natural log of centroid size (Fig. 7B), represents an ontogenetic trajectory for all fish in this study and allows visualization of a phenomenon unique to the freshwater dataset. Wild-caught adults from this habitat are smaller than younger lab-reared fish whose parents originated from this habitat. This size discrepancy was not observed for the habitats, where age and size remain positively correlated throughout. The Roquefeuil Bay marine population is also notable for having a flatter slope than the other habitats and a trajectory that crosses that of the Roquefeuil Bay marine group. Finally, the Roquefeuil Bay marine trajectory is substantially longer in this representation, indicating the presence of a much greater range of specimen sizes than in the other two groups. The freshwater trajectory is vertically displaced, and is shorter than those of the other two groups.

DISCUSSION

Differences among complex phenotypes are evident early in ontogeny

Parallel morphological divergence among stickleback occupying habitats that diverge on a micro scale [e.g. benthic–limnetic (Lavin and McPhail, 1987; Willacker *et al.*, 2010)] or a macro scale [e.g. marine–freshwater (Bell and Foster, 1994; Aguirre and Bell, 2012)] has been extensively studied, and our understanding of this phenomenon contributed substantially to the theoretical conceptualization of adaptive radiation and ecological speciation (Schluter and Nagel, 1995; Schluter,

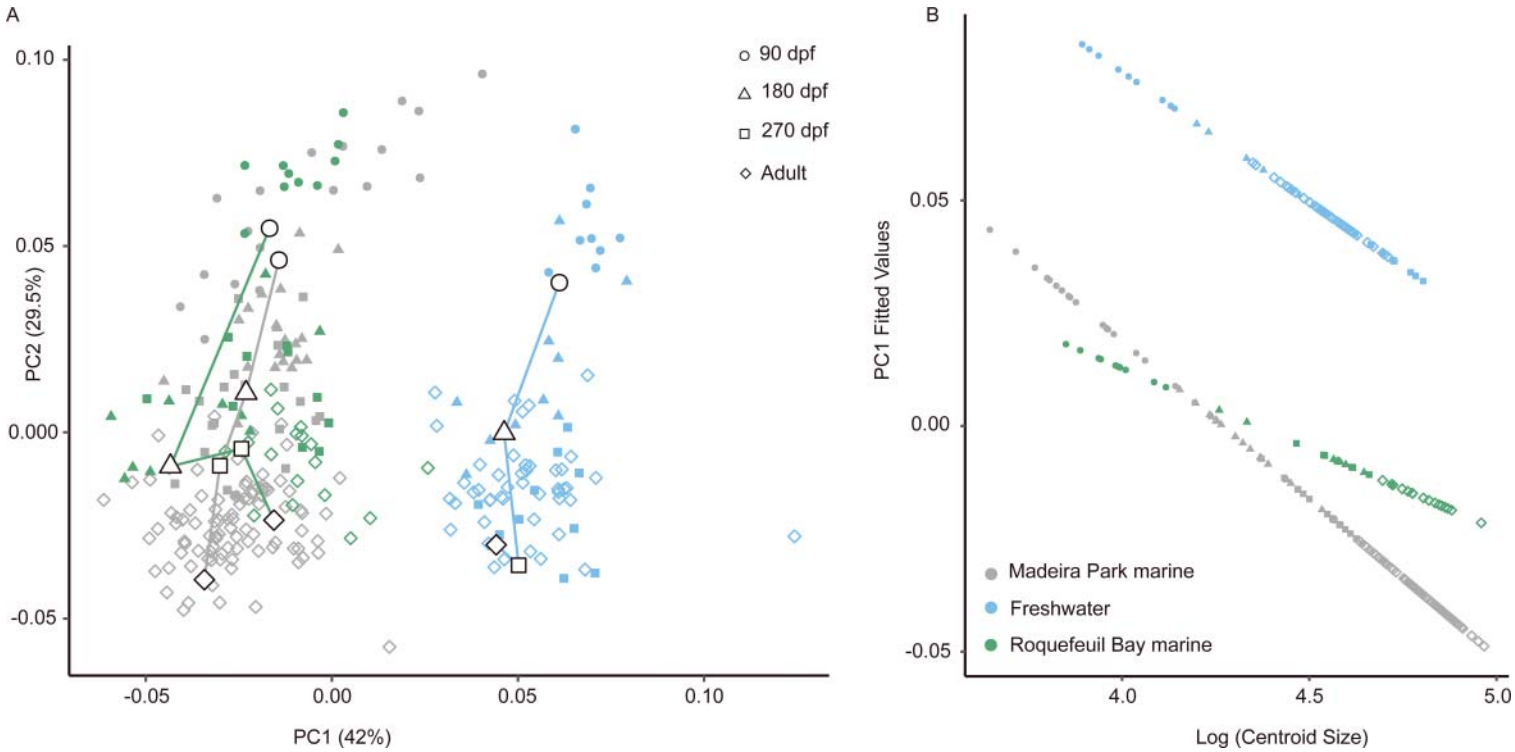

Fig. 7. Trajectory analysis and whole-dataset allometric trends. Small shapes indicate individuals; large shapes indicate mean shape at each age. Abbreviations: dpf = days post-fertilization; Log = natural log; PC = principal component.

2000; Schluter *et al.*, 2010). Understanding when in development this divergence occurs is key to deciphering the means by which environment and genotype interact to structure phenotypic variation, and which gene pathways are responsible for the production of this variation and therefore of particular interest for the study of natural selection (Hallgrimsson *et al.*, 2012). Here we demonstrate that significant differences among Madeira Park and Roquefeuil Bay marine and freshwater forms of *G. aculeatus* are already present by 90 days post-fertilization (dpf). At this time point, freshwater fish exhibit many of the features of what has been described as the 'limnetic' freshwater phenotype (McPhail, 1984; Caldecutt and Adams, 1998), including a large orbit [but see Willacker *et al.* (2010) for a contrasting result], a relatively fusiform skull shape, and upturned oral jaws. Freshwater fish also have both shorter and substantially more gracile pelvic spines than marine fish. These differences persist across the entire ontogenetic series documented here. The pelvic spines are particularly interesting in that fish at 90 dpf differ less than do older stages for this feature. This difference may be related to the development of secondary sexual characteristics as fish mature, as pelvic spine morphology is known to be sexually dimorphic in *G. aculeatus* (Reimchen *et al.*, 2016).

It is also interesting to note that differences between Madeira Park marine and freshwater phenotypes are stronger than any other pairwise comparison throughout this dataset despite their geographic proximity, and that the Madeira Park marine individuals occupy substantially more morphospace than the other two groups until they reach adulthood. A second interesting result of this study is that upon reaching adult morphology, it is clear that there are significant differences among marine individuals as well as between these and the freshwater individuals, despite raising all specimens included here in a common freshwater environment. This result suggests that genetic differences underlie the observed phenotypic differences, and contributes to the growing body of evidence (Morris *et al.*, 2018; T.N. Barry *et al.*, in prep.), suggesting the choice of population in studies requiring a representative ancestral form of *G. aculeatus* is important. Likely not all marine populations are equally appropriate in this context, even if sampled in geographic proximity. Further, the finding that marine populations differ substantively suggests the possibility that fully marine and freshwater forms are both derived conditions from a putatively ancestral Madeira Park marine phenotype; in other words, that contemporary marine stickleback continue to evolve and, to some extent, diverge from each other and should not be considered representative of an ancestral phenotype. Our results also indicate strongly increased phenotypic variance in the Madeira Park marine sample raised in fresh water, which provides support for the finding that the presence of a 'flexible stem' (Wund *et al.*, 2008) may be contributing to *G. aculeatus*' capacity to adapt to changing environments, although the role of plasticity in structuring phenotypic variance was not directly tested here. Further work will require a more thorough characterization of the capacity of various types of marine stickleback populations to colonize freshwater habitats to test these hypotheses.

Ontogenetic trajectories indicate different sources of adaptive variation between habitats and within replicate habitats

When comparing ontogenetic trajectories among groups, it is important to note that while differences may occur in length and direction of the total trajectory, they may also occur in the shape present in each group at the beginning of the trajectory. The starting point for a particular trajectory may occur at a different elevation relative to another, resulting in parallel trajectories, or may be shifted relative to another, resulting in overlapping

trajectories (Sheets and Zelditch, 2013). Changes in trajectory origin indicate the relative contribution of inherited information and developmental timing to trajectory outcomes. Our data reveal that fish from marine and freshwater habitats already possess established differences in habitat specific phenotype, as indicated by the differences in starting point visualized in Fig. 7A and 7B. Whether considered in a two-dimensional representation of morphospace (Fig. 7A) or in a more traditional shape-by-size ontogenetic representation (Fig. 7B), it is apparent that the fish from the freshwater habitat are already different in shape at 90 dpf (confirmed by statistical analysis, Table 2), which may indicate that selection at earlier life stages has already produced differentiation among phenotypes (Sheets and Zelditch, 2013), with such differences arising either from inherited information or from alterations in developmental timing (Klingenberg, 1998).

As depicted in Fig. 7B, the ontogenetic trajectory observed for the freshwater population never crosses those of the marine groups, and follows an essentially parallel trajectory to that of the Madeira Park marine habitat. The Madeira Park marine trajectory indicates some evidence of alteration in developmental timing with respect to the Roquefeuil Bay marine trajectory, with its origin displaced slightly along their initially converging trajectories (Klingenberg, 1998). Convergent trajectories such as these are thought to indicate the presence of functional constraints, induced by aspects of habitat or diet, that appear despite inherited morphological differences that separate trajectories in space (Adams and Nistri, 2010; Simonsen *et al.*, 2017). These trajectories continue to diverge after crossing, and Fig. 7A indicates a displacement in morphospace between 180 and 270 dpf that positions the final Roquefeuil Bay marine phenotype intermediate to the freshwater and Madeira Park marine forms. This pattern indicates that although convergent functional constraints exist in marine environments, Roquefeuil Bay marine fish may also be subject to selective forces that bias their phenotype towards a different adaptive peak from a common shared 'marine-like' phenotype present at earlier life stages, indicated here by proximity of marine morphospaces relative to the freshwater morphospace throughout development. A previous study documenting ontogeny of whole-body shape in adult and sub-adult (35–50 mm SL) *G. aculeatus* (Spoljaric and Reimchen, 2011) revealed that marine and freshwater populations have opposite relationships between shape and size. Here we found that shape–size trajectories followed the same orientation across ontogeny, but also found substantial variation in this relationship within each age, documenting a pattern similar to that reported by Spoljaric and Reimchen (2011) at sexual maturity. Our study encompassed a greater range of size and age, and the variation present in the relationship between size and shape over time may indicate the presence of key developmental periods in which timing changes are contributing to eventual adult morphologies.

Taken together, these results provide intriguing evidence of the means by which marine sticklebacks representing different habitat subtypes, and freshwater sticklebacks attain their divergent adult morphologies. We show that significant variation between Madeira Park and Roquefeuil Bay marine forms may be due in part to heterochronic effects on a conserved morphology through ontogeny followed by modulation due to functional constraints experienced by adult fish in different marine habitats. In contrast, the striking differences present between freshwater and marine forms are already established early in development, likely due to a combination of inherited and environmental influences, and these differences are reinforced across ontogeny such that marine and freshwater adults remain vastly different. Intriguingly, these results are consistent with those of a recent study focusing on the earlier portion of *G. aculeatus* ontogeny and on the development of individual skeletal

elements rather than complex phenotypes (Currey *et al.*, 2017). This study focused on time points earlier than those presented here (7–50 dpf), and found evidence for phenotypic divergence between marine and freshwater forms to be consistent with the presence of a genetic basis for these trait differences, as suggested by the difference in trajectory origin point reported here. In contrast to our study, Currey *et al.* (2017) compared two freshwater habitats to one putatively ancestral marine habitat, but they also noted that divergence in bony elements between representatives of the two freshwater habitats was due to changes in developmental timing. This is also consistent with our finding that ontogenetic trajectory variation among fish from more similar habitats (Madeira Park and Roquefeuil Bay marine) is largely produced via heterochronic shifts and functional constraints on adult morphology, whereas differences among fish from more divergent habitats (freshwater and marine) has a stronger genetic basis.

Our results therefore suggest, by combining evidence obtained from both trajectory analysis and examination of shape changes during ontogeny, the hypothesis that genetic differentiation is responsible for the large divergence between marine and freshwater *G. aculeatus* in this system, whereas heterochronic shifts may be responsible for the smaller divergence between marine subtypes. Recent work has shown that there exists considerable, largely undocumented phenotypic and genetic variation among marine *G. aculeatus* along the Pacific coast (Morris *et al.*, 2018), and developmental differences among marine forms have also been documented (Wund *et al.*, 2012). Testing this hypothesis will require further documentation of gene flow among these populations in order to determine the degree to which they are isolated from each other, and the relative contributions of developmental timing and genetic information to the differences observed. It should also be noted here that the juvenile specimens studied here are F1 offspring, and it is possible that maternal effects may be playing a role. It will be important to consider such effects (and other epigenetic contributions) in future work.

The retention of size in the consideration of shape in these analyses is a source of controversy in the literature, where many studies have sought to control for size through the application of group-centred regression followed by comparisons of regression residuals. Here we prefer to consider size as an integral part of organism shape, and we suggest that rather than obscuring shape differences, the inclusion of size explicitly in these analyses helps to better elucidate the relationship between size and shape in evolution. For example, the wild-caught adult Klein Lake fish included here are smaller than many of the 180 and 270 dpf animals produced from crosses of these wild adults, an observation that did not extend to the marine habitats. Although wild freshwater *G. aculeatus* are often (although not always) smaller than wild marine fish, our results suggest that constraints related to habitat, possibly including the availability of prey or the nutritional density of available prey items, may be constraining growth in the wild. When raised in a laboratory environment where prey availability is not limited, freshwater *G. aculeatus* are able to attain a much larger size. Previous work has also indicated an effect of rearing environment on allometric trajectories in *G. aculeatus* (Wund *et al.*, 2012). This is of particular interest because in many studies of *G. aculeatus*, reproductive maturity is determined by the attainment of a standard length of at least 35 mm. This study suggests that size may be more labile than previously appreciated, and that the use of size to determine sexual maturity may be unreliable. More broadly, this result indicates that laboratory rearing does not sufficiently replicate the wild environment for *G. aculeatus*, and that the effects of laboratory rearing on phenotype should be considered in future work.

The comparison of wild-caught adults with laboratory-reared juveniles is one of several limitations in this study. Future work should ideally consider complete ontogenetic series from a single rearing condition, either wild or laboratory. Furthermore, sex ratios in the adult sample are biased towards females, with a paucity of male specimens particularly apparent in the Roquefeuil Bay marine group, limiting our ability to discuss sexual dimorphism explicitly. Several possible reasons for this bias exist, as reported by others for *G. aculeatus* (e.g. Confer *et al.*, 2012). Wild sampling for this work occurred during May and June only, and it is possible that sampling with minnow traps during the peak reproductive season for *G. aculeatus* produced female-centric sampling bias. It is also possible that our sampling window covered the period in which male fish were tending nests and thus were relatively stationary, with the consequence that they were under-represented in minnow traps. Finally, our results point to a need for inclusion of ecological replicates, and future work should consider sampling multiple freshwater and marine localities at different times throughout the year in order to mitigate these biases.

Our intention in this study was to consider the whole skeleton in three dimensions, and we therefore chose to begin sampling at 90 dpf. While the major bony elements of *G. aculeatus* are present by 50 dpf (Swarup, 1958), work in our laboratory has indicated that ossification remains incomplete until at least 60 dpf and often longer (Pistore, 2017). As a result of this approach, the most important limitation in this study became apparent only after the work was complete, namely that phenotypic differences between marine and freshwater *G. aculeatus* are already established in the skeleton by our first sample time point at 90 dpf. Although previous studies have produced important information using histological techniques to visualize ossifying elements in two dimensions (e.g. Currey *et al.*, 2017), our intention was to consider the skeleton as a whole using a three-dimensional approach, which required near-complete ossification to achieve. In order to better capture the origination of phenotypic differences as we describe them here, future work will need to extend to earlier developmental stages that are able to capture early three-dimensional phenotypes more effectively [e.g. optical projection tomography (Sharpe, 2003)] and cover the entire ontogenetic trajectory of each habitat from fertilization to reproductive maturity.

ACKNOWLEDGEMENTS

We are grateful for research support from the Bamfield Marine Sciences Centre that made this work possible. We thank S. Vamosi, M. Morris, C. Zurowski, and J. Theodor for technical assistance, and S. Vamosi, J. Bertram, L. Jackson, and the Jamniczky and Rogers group members for helpful discussions and comments. We gratefully acknowledge two anonymous reviewers, whose comments helped to improve the quality of this contribution. This research was funded by Natural Sciences and Engineering Research Council of Canada Discovery grants to S.M.R. and H.A.J.

REFERENCES

Adams, D.C. and Collyer, M.L. 2009. A general framework for the analysis of phenotypic trajectories in evolutionary studies. *Evolution*, **63**: 1143–1154.

Adams, D.C. and Nistri, A. 2010. Ontogenetic convergence and evolution of foot morphology in European cave salamanders (Family: Plethodontidae). *BMC Evol. Biol.*, **10**: 216. Available at: https:/doi.org/10.1186/1471-2148-10-216.

Adams, D.C., Collyer, M.L. and Kaliontzopoulou, A. 2018. *Geomorph: Software for geometric morphometric analyses*. R package version 3.0.6.

Aguirre, W.E. and Bell, M.A. 2012. Twenty years of body shape evolution in a threespine stickleback population adapting to a lake environment. *Biol. J. Linn. Soc.*, **105**: 817–831.

Albert, A.Y.K., Sawaya, S., Vines, T.H., Knecht, A.K., Miller, C.T., Summers, B.R. *et al.* 2008. The genetics of adaptive shape shift in stickleback: pleiotropy and effect size. *Evolution*, **62**: 76–85.

Barrett, R.D.H., Rogers, S.M. and Schluter, D. 2008. Natural selection on a major armor gene in threespine stickleback. *Science*, **322**: 255–257.

Bell, M.A. 1976. Evolution of phenotypic diversity in *Gasterosteus aculeatus* superspecies on the Pacific coast of North America. *Syst. Zool.*, **25**: 211–227.

Bell, M.A. and Foster, S.A., eds. 1994. *The Evolutionary Biology of the Threespine Stickleback*. New York: Oxford University Press.

Caldecutt, W.J. and Adams, D.C. 1998. Morphometrics of trophic osteology in the threespine stickleback, *Gasterosteus aculeatus*. *Copeia*, **1998**: 827–838.

Collyer, M.L. and Adams, D.C. 2013. Phenotypic trajectory analysis: comparison of shape change patterns in evolution and ecology. *Hystrix*, **24**: 75–83.

Collyer, M.L., Sekora, D.J. and Adams, D.C. 2015. A method for analysis of phenotypic change for phenotypes described by high-dimensional data. *Heredity*, **115**: 357–365.

Collyer, M.L., Adams, D.C. and Freckleton, R. 2018. RRPP: An r package for fitting linear models to high-dimensional data using residual randomization. *Meth. Ecol. Evol.*, **9**: 1772–1779.

Colosimo, P.F., Hosemann, K.E., Balabhadra, S., Villareal, G., Jr., Dickson, M., Grimwood, J. *et al.* 2005. Widespread parallel evolution in sticklebacks by repeated fixation of ectodysplasin alleles. *Science*, **307**: 1928–1933.

Confer, A., Vu, V. and Aguirre, W.E. 2012. Occurrence of *Schistocephalus solidus* in anadromous threespine stickleback. *J. Parasitol.*, **98**: 676–678.

Currey, M.C., Bassham, S., Perry, S. and Cresko, W.A. 2017. Developmental timing differences underlie armor loss across threespine stickleback populations. *Evol. Dev.*, **19**: 231–243.

Dryden, I.L. and Mardia, K.V. 1998. *Statistical Shape Analysis*. New York: Wiley.

Green, R.M., Fish, J.L., Young, N.M., Smith, F.J., Roberts, B., Dolan, K. *et al.* 2017. Developmental nonlinearity drives phenotypic robustness. *Nat. Commun.*, **8**: 1970. Available at: https://doi.org/10.1038/s41467-017-02037-7.

Grush, J., Noakes, D.L.G. and Moccia, R.D. 2004. The efficacy of clove oil as an anesthetic for the zebrafish, *Danio rerio* (Hamilton). *Zebrafish*, **1**: 46–53.

Hagen, D.W. and Gilbertson, L.G. 1972. Geographic variation and environmental selection in *Gasterosteus aculeatus* L. in the Pacific Northwest, America. *Evolution*, **26**: 32–51.

Hallgrimsson, B., Jamniczky, H.A., Young, N.M., Rolian, C., Schmidt-Ott, U. and Marcucio, R.S. 2012. The generation of variation and the developmental basis for evolutionary novelty. *J. Exp. Zool.*, **318**: 501–517.

Hendrikse, J.L., Parsons, T.E. and Hallgrimsson, B. 2007. Evolvability as the proper focus of evolutionary developmental biology. *Evol. Dev.*, **9**: 393–401.

Jamniczky, H.A., Barry, T.N. and Rogers, S.M. 2015. Eco-evo-devo in the study of adaptive divergence: examples from threespine stickleback (*Gasterosteus aculeatus*). *Integr. Comp. Biol.*, **55**: 166–178.

Jones, F.C., Grabherr, M.G., Chan, Y.F., Russell, P., Mauceli, E., Johnson, J. *et al.* 2012. The genomic basis of adaptive evolution in threespine sticklebacks. *Nature*, **484**: 55–61.

Klingenberg, C.P. 1998. Heterochrony and allometry: the analysis of evolutionary change in ontogeny. *Biol. Rev.*, **73**: 79–123.

Lavin, P.A. and McPhail, J.D. 1987. Morphological divergence and the organization of trophic characters among lacustrine populations of the threespine stickleback (*Gasterosteus aculeatus*). *Can. J. Fish. Aquat. Sci.*, **44**: 1820–1829.

Lewontin, R.C. 1974. *The Genetic Basis of Evolutionary Change*. New York: Columbia University Press.

McPhail, J.D. 1984. Ecology and evolution of sympatric sticklebacks (*Gasterosteus*): morphological and genetic evidence for a species pair in Enos Lake, British Columbia. *Can. J. Zool.*, **62**: 1402–1408.

McPhail, J.D. 1993. Ecology and evolution of sympatric sticklebacks (*Gasterosteus*): origin of the species pairs. *Can. J. Zool.*, **71**: 515–523.

Miller, C.T., Glazer, A.M., Summers, B.R., Blackman, B.K., Norman, A.R., Shapiro, M.D. *et al.* 2014. Modular skeletal evolution in sticklebacks is controlled by additive and clustered quantitative trait loci. *Genetics*, **197**: 405–420.

Morris, M.R.J., Bowles, E., Allen, B.E., Jamniczky, H.A. and Rogers, S.M. 2018. Contemporary ancestor? Adaptive divergence from standing genetic variation in Pacific marine threespine stickleback. *BMC Evol. Biol.*, **18**: 113. Available at: https://doi.org/10.1186/s12862-018-1228-8.

Peichel, C.L., Nereng, K.S., Ohgi, K.A., Cole, B.L.E., Colosimo, P.F., Buerkle, C.A. *et al.* 2001. The genetic architecture of divergence between threespine stickleback species. *Nature*, **414**: 901–905.

Peichel, C.L., Ross, J.A., Matson, C.K., Dickson, M., Grimwood, J., Schmutz, J. *et al.* 2004. The master sex-determination locus in threespine sticklebacks is on a nascent Y chromosome. *Curr. Biol.*, **14**: 1416–1424.

Peichel, C.L., Sullivan, S.T., Liachko, I. and White, M.A. 2017. Improvement of the threespine stickleback genome using a Hi-C-based proximity-guided assembly. *J. Hered.*, **108**: 693–700.

Pistore, A.E. 2017. *Ontogeny of population-specific phenotypic variation in the Threespine Stickleback*. Masters thesis, University of Calgary.

R Core Team. 2016. *RStudio: Integrated Development for R*. Boston, MA: RStudio.

R Core Team. 2018. *R: A Language and Environment for Statistical Computing*. Vienna, Austria: R Foundation for Statistical Computing.

Reimchen, T.E., Steeves, D. and Bergstrom, C.A. 2016. Sex matters for defence and trophic traits of threespine stickleback. *Evol. Ecol. Res.*, **17**: 459–485.

Rennison, D.J., Heilbron, K. and Barrett, R.D. 2015. Discriminating selection on lateral plate phenotype and its underlying gene, *Ectodysplasin*, in threespine stickleback. *Am. Nat.*, **185**: 150–156.

Schluter, D. 1996. Adaptive radiation along genetic lines of least resistance. *Evolution*, **50**: 1766–1774.

Schluter, D. 2000. *The Ecology of Adaptive Radiation*. Oxford: Oxford University Press.

Schluter, D. and Nagel, L.M. 1995. Parallel speciation by natural selection. *Am. Nat.*, **146**: 292–301.

Schluter, D., Marchinko, K.B., Barrett, R.D.H. and Rogers, S.M. 2010. Natural selection and the genetics of adaptation in threespine stickleback. *Phil. Trans. R. Soc. Lond. B: Biol. Sci.*, **365**: 2479–2486.

Schmalhausen, I.I. 1949. *Factors of Evolution*. Philadelphia, PA: The Blackiston Company.

Sharpe, J. 2003. Optical projection tomography as a new tool for studying embryo anatomy. *J. Anat.*, **202**: 175–181.

Sheets, H.D. and Zelditch, M.L. 2013. Studying ontogenetic trajectories using resampling methods and landmark data. *Hystrix*, **24**: 67–73.

Simonsen, M.K., Siwertsson, A., Adams, C.E., Amundsen, P.A., Praebel, K. and Knudsen, R. 2017. Allometric trajectories of body and head morphology in three sympatric Arctic charr (*Salvelinus alpinus* (L.)) morphs. *Ecol. Evol.*, **7**: 7277–7289.

Spoljaric, M.A. and Reimchen, T.E. 2011. Habitat-specific trends in ontogeny of body shape in stickleback from coastal archipelago: potential for rapid shifts in colonizing populations. *J. Morphol.*, **272**: 590–597.

Swarup, H. 1958. Stages in the development of the stickleback *Gasterosteus aculeatus* (L.). *Development*, **6**: 373–383.

Walker, J.A. 1997. Ecological morphology of lacustrine threespine stickleback *Gasterosteus aculeatus* L. (Gasterosteidae) body shape. *Biol. J. Linn. Soc.*, **61**: 3–50.

Wickham, H. 2011. The split-apply-combine strategy for data analysis. *J. Stat. Softw.*, **40**: 1–29.
Willacker, J.J., von Hippel, F.A., Wilton, P.R. and Walton, K.M. 2010. Classification of threespine stickleback along the benthic–limnetic axis. *Biol. J. Linn. Soc.*, **101**: 595–608.
Wund, M.A., Baker, J.A., Clancy, B., Golub, J.L. and Foster, S.A. 2008. A test of the 'flexible stem' model of evolution: ancestral plasticity, genetic accommodation, and morphological divergence in the threespine stickleback radiation. *Am. Nat.*, **172**: 449–462.
Wund, M.A., Valena, S., Wood, S. and Baker, J.A. 2012. Ancestral plasticity and allometry in threespine stickleback fish reveal phenotypes associated with derived, freshwater ecotypes. *Biol. J. Linn. Soc.*, **105**: 573–583.